

# Maximizing Field-Effect Mobility and Solid-State Luminescence in Organic Semiconductors\*\*

Afshin Dadvand, Andrey G. Moiseev, Kosuke Sawabe, Wei-Hsin Sun, Brandon Djukic, Insik Chung, Taishi Takenobu, Federico Rosei, and Dmitrii F. Perepichka\*

Tunable multifunctional properties that are accessible through synthetic design and facilitated device fabrication are the key advantages of organic semiconductors (OSCs) as optoelectronic materials. A tandem of light-emitting and charge-transporting properties in OSCs has been widely explored, and already commercialized in organic light-emitting diodes (OLEDs) and displays.<sup>[1,2]</sup> At the same time, it proved to be very difficult to maximize the charge mobility ( $\mu$ ) and luminescence efficiency in the same OSCs. As a result of a short electrical channel length, OLEDs do not require a  $\mu$  value of more than  $10^{-4}$ – $10^{-2}$  cm<sup>2</sup> V<sup>-1</sup> s<sup>-1</sup>, however, a number of technological opportunities could arise if highly emissive OSCs with a  $\mu$  value of more than 1 cm<sup>2</sup> V<sup>-1</sup> s<sup>-1</sup> were available. These include organic light-emitting transistors (OLETs),<sup>[3]</sup> which combine the electroluminescence (EL) with the current-control function of a field-effect transistor (FET), and potentially allow simplifying the structure of active matrix displays. Larger current densities that are attainable in transistor configurations (versus that in OLEDs<sup>[3d]</sup>) are highly desirable for the development of electrically pumped organic lasers.<sup>[4]</sup> However, this demands new materials with high  $\mu$  value.

Achieving a  $\mu$  value of greater than 1 cm<sup>2</sup> V<sup>-1</sup> s<sup>-1</sup> in OSCs generally requires crystalline materials with strong  $\pi$ – $\pi$  interactions. However, such interactions most often lead to suppression of luminescence in the solid state.<sup>[5]</sup> Nearly all

efficient electroluminescent organic materials are amorphous. There are several reasons for luminescence quenching in the solid state, which include fission of a singlet exciton to give two non-emissive triplets,<sup>[6]</sup> as well as exciton quenching on the defect sites. On the other hand, some conjugated molecules, for example, tetraarylethylenes,<sup>[7]</sup> show enhancement of photoluminescence (PL) in the solid state (aggregation-enhanced emission).<sup>[8]</sup> One of the simplest blue emitters, anthracene, has a PL quantum yield (PLQY) of 64 % in crystals,<sup>[9]</sup> but no thin-film transistors have been produced from this material. The larger aromatic core in tetracene gives rise to reasonable charge mobility of approximately 0.1 cm<sup>2</sup> V<sup>-1</sup> s<sup>-1</sup> in thin-film FETs,<sup>[10]</sup> but the solid-state PLQY drops down to 0.8 %, mostly as a result of singlet fission.<sup>[11]</sup> The tetraphenyl derivative of tetracene, rubrene, has a large FET mobility of up to 10–20 cm<sup>2</sup> V<sup>-1</sup> s<sup>-1</sup> in single crystals<sup>[12]</sup> but a correspondingly very low (less than 1 %) PLQY in the solid state, which is also attributed to singlet fission.<sup>[6b]</sup> Pentacene, a benchmark *p*-type OSC has a mobility above 1.0 cm<sup>2</sup> V<sup>-1</sup> s<sup>-1</sup><sup>[13]</sup> and does not fluoresce in the solid state. A number of other high-mobility OSCs have been reported,<sup>[14]</sup> including dinaphthothienothiophene and its derivatives, with a  $\mu$  value of 8 cm<sup>2</sup> V<sup>-1</sup> s<sup>-1</sup> or less in thin films<sup>[15]</sup> and 16 cm<sup>2</sup> V<sup>-1</sup> s<sup>-1</sup> in single crystals.<sup>[16]</sup> However, these compounds all have low or no emission in the solid state. The overall picture emerging from the literature is that maximizing the charge mobility in OSCs necessarily leads to decreased emission efficiency.

Herein, we show that a charge mobility of greater than 1 cm<sup>2</sup> V<sup>-1</sup> s<sup>-1</sup> can be achieved in a structurally simple OSC that also produces blue EL and PL with a PLQY of 70 % in the crystalline state. Recently, styrylacenes have emerged as a promising subclass of OSC, in which extending the conjugation through the styrene group and keeping the less-stable acene moiety short allows a high field-effect mobility together with good stability to be achieved.<sup>[17]</sup> We reported a green-emitting OLET that is based on 2-(4-pentylphenylvinyl)tetracene (PPVTet).<sup>[17c]</sup> Although a reasonable hole mobility (ca. 0.2 cm<sup>2</sup> V<sup>-1</sup> s<sup>-1</sup>) was measured in these devices, PPVTet has a low solid-state PLQY of approximately 7 %. In this study, we report the surprising finding that shrinking the acene moiety (from tetracene to anthracene) leads to a new OSC, 2-(4-hexylphenylvinyl)anthracene (HPVant), that has an even higher charge mobility, and a solid-state PLQY of 70 %. These are the key properties for the development of high-current light-emitting devices, and we demonstrate a blue-emitting OLET based on HPVant.

HPVant was synthesized from 2-hydroxyanthraquinone (**1**) by reducing **1** with NaBH<sub>4</sub>, activating the hydroxy group of

[\*] A. Dadvand, Dr. A. G. Moiseev, W.-H. Sun, Dr. B. Djukic, I. Chung, Prof. D. F. Perepichka  
Department of Chemistry and Centre for Self-Assembled Chemical Structures, McGill University  
801 Sherbrooke Street West, H3A 2K6 Montreal, QC (Canada)  
E-mail: dmitrii.perepichka@mcgill.ca

A. Dadvand, Prof. F. Rosei  
INRS—Énergie, Matériaux et Télécommunications (Canada)

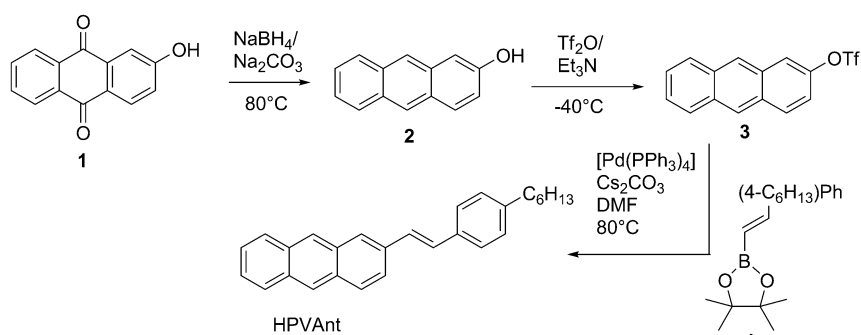
K. Sawabe  
Department of Physics, Graduate School of Science  
Tohoku University (Japan)

K. Sawabe, Prof. T. Takenobu  
Graduate School of Advanced Science and Engineering  
Waseda University (Japan)

[\*\*] This work was funded by the NSERC of Canada through Discovery Grants and a CRD grant supported by Plasmionique Inc. We are grateful to the CFI and NSERC for infrastructure support. F.R. acknowledges the Canada Research Chairs program for partial salary support. We acknowledge Prof. G. Hanan and F. Belanger (University of Montreal) for access to lifetime measurements and X-ray analysis, respectively.



Supporting information for this article is available on the WWW under <http://dx.doi.org/10.1002/anie.201108184>.



**Scheme 1.** Synthesis of HPVAnt. Tf = trifluoromethanesulfonyl; DMF = *N,N*-dimethylformamide.

anthracene (**2**) with triflic anhydride and, finally, a Suzuki coupling of the resulting triflate **3** with 4-hexylphenylvinylboronic ester **4** (Scheme 1). As a result of the small acene core and lack of reactive moieties, HPVAnt has high thermal and chemical stability.

Density functional theory (DFT) calculations at the B3LYP/6-31G(d) level in the gas phase predict the HOMO and LUMO of HPVAnt at  $-5.05$  eV and  $-1.78$  eV, respectively (see the Supporting Information). The HOMO and LUMO of HPVAnt as measured electrochemically in solution are  $-5.47$  eV and  $-2.57$  eV, respectively (assuming ferrocene at  $-4.80$  eV, see the Supporting Information). The absorption spectrum of HPVAnt in solution has a vibronically structured band with peaks at  $\lambda_{\text{max}} = 362, 378$ , and  $397$  nm (Figure 1). The optical gap determined from the onset of this band ( $3.0$  eV,  $410$  nm) is in reasonable agreement with the value measured electrochemically ( $2.9$  eV) and DFT calculations ( $3.27$  eV). The PL spectrum is also vibronically structured ( $\lambda_{\text{max}} = 422, 438$ , and  $479$  nm). Both absorption and emission are red-shifted in the solid state, and the band gap determined from an onset absorption is  $2.8$  eV. The high absolute PLQY of 70% measured in an integrating sphere in single crystals (up from 55% in solution) makes HPVAnt a good candidate for OLET applications; a lower PLQY of approximately 20%

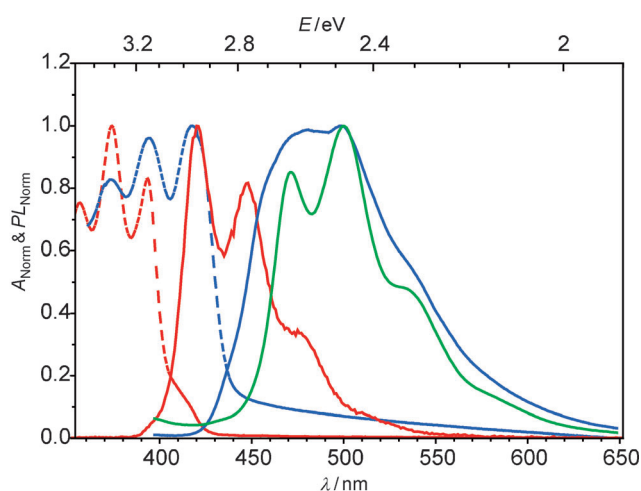


**Figure 1.** Absorption (broken lines) and PL ( $\lambda_{\text{ex}} = 410$  nm, solid lines) spectra of HPVAnt in solution ( $2 \times 10^{-5}$  M in toluene, red), as a thin film (on quartz, blue), and as a single crystal (teal).<sup>[28]</sup>

was measured in thin films, which is likely a result of exciton quenching on surface defects.<sup>[18]</sup> The same trend was reported for anthracene, which has a PLQY of 64%, 28%, and 18% in single crystal, solution, and powder forms, respectively.<sup>[9]</sup>

We suggest that the high PLQY of HPVAnt crystals might result from the cessation of the singlet-fission process. Indeed, time-dependent DFT calculations (see the Supporting Information) predict that the energy of singlet exciton  $S_1$  of styrylanthracene ( $3.04$  eV) is insufficient for generating two triplets

( $T_1 = 1.74$  eV). The calculations are in agreement with the spectroscopically determined  $S_1$  state ( $2.94$ – $3.15$  eV<sup>[19]</sup>) and the reported triplet energy of  $1.77$  eV for 2-(4-methylphenylvinyl)anthracene,<sup>[20]</sup> which confirms the endothermic nature of singlet fission and explains the high PLQY of HPVAnt crystals. In contrast, the  $S_1$  energy ( $2.39$  eV) of the tetracene derivative PPVTet (discussed above) matches the energy of two triplets ( $T_1 = 1.20$  eV), which enables single fission and explains its low PLQY. Analysis of published photophysical data and DFT calculations reveal the same trend ( $S_1 \geq 2T_1$ ) for other high-mobility acene OSCs, including tetracene,<sup>[6a]</sup> pentacene,<sup>[6a]</sup> and rubrene.<sup>[21]</sup> Accordingly, all of these suffer luminescence quenching in the solid state.

The transistor properties of HPVAnt were studied in thin films (TF) and single crystals (SC) in top-contact configuration (Figure 2). Typical output and transfer characteristics of the TF-FET that is based on HPVAnt are shown in Figure 2c and d. Remarkably, without any device optimization, HPVAnt films grown on bare Si/SiO<sub>2</sub> at room temperature have an average hole mobility  $\mu^+$  value of  $(1.14 \pm 0.2) \text{ cm}^2 \text{ V}^{-1} \text{ s}^{-1}$  with a threshold voltage ( $V_T$ ) of  $-20$  to  $-24$  V and an on/off ratio of  $10^6$ – $10^7$ . The highest  $\mu^+$  value that was measured in these devices was  $1.5 \text{ cm}^2 \text{ V}^{-1} \text{ s}^{-1}$ . We note

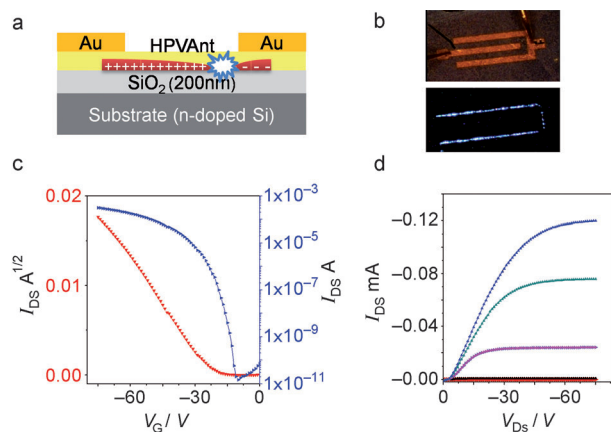


**Figure 2.** Top-contact TF-FET fabricated with HPVAnt: a) Schematic and b) optical image and EL of the biased device. c) Transfer characteristics of the biased device.  $V_{\text{DS}} = -75$  V d) Output characteristics of the biased device.  $V_{\text{G}} = -75$  V (blue);  $-60$  V (teal);  $-45$  V (pink);  $-30$  V (black);  $-15$  V (red);  $\mu = 1.33 \text{ cm}^2 \text{ V}^{-1} \text{ s}^{-1}$ ; on/off =  $3 \times 10^7$ ;  $V_T = -24$  V.  $I_{\text{DS}}$  is drain-source current.

that the mobility of HPVAnt slightly exceeded that of similar pentacene-based devices fabricated by us, despite the higher calculated reorganization energy of the HPVAnt-based devices ( $\lambda_{0/+} = 0.18$  eV versus 0.09 eV for pentacene,<sup>[22]</sup> see the Supporting Information). A somewhat lower mobility was measured for TF-FETs that were fabricated on Si/SiO<sub>2</sub> modified with hexamethyldisilazane (HMDS,  $(0.8 \pm 0.1) \text{ cm}^2 \text{ V}^{-1} \text{ s}^{-1}$ ) or poly(methyl methacrylate) (PMMA,  $(0.45 \pm 0.08) \text{ cm}^2 \text{ V}^{-1} \text{ s}^{-1}$ ) layers. This can likely be ascribed<sup>[23]</sup> to the rougher nature of these surfaces (root mean squared (RMS) of 0.18 nm for bare Si/SiO<sub>2</sub> and 0.45 nm for PMMA-coated Si/SiO<sub>2</sub>).

The high mobility in TF-FET benefits from the almost perfect layer-by-layer growth at room temperature, which leads to continuous OSC films at a low nominal thickness, as confirmed by atomic force microscopy (AFM, Figure 3). The height profile suggests an upright orientation of molecules in

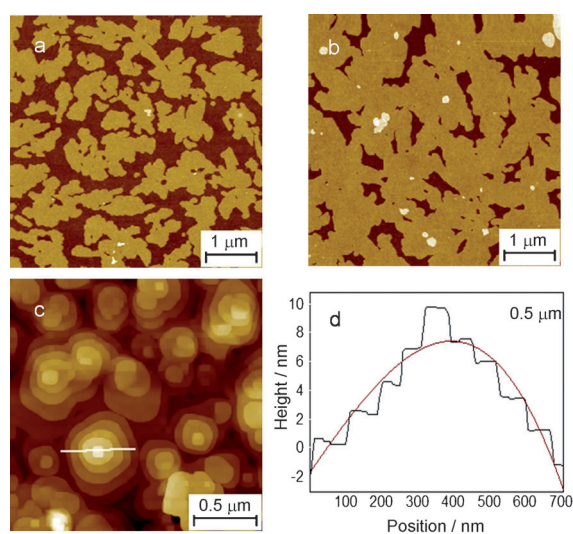


**Figure 3.** AFM images of a) submonolayer, b) monolayer, and c) multi-layer films of HPVAnt grown on Si/SiO<sub>2</sub>. d) Height profile of image (c).

the layers. X-ray diffraction analysis of the vacuum-deposited films corresponds well to that of bulk HPVAnt powder (see the Supporting Information). Although the single-crystal X-ray diffraction data are of insufficient quality to deduce the exact interatomic distances, the orientation of the molecules in the unit cell is clear (see the Supporting Information) and closely resembles that of 2,6-bis(4-pentylphenylvinyl)anthracene.<sup>[17a]</sup> The molecules pack in a usual herringbone fashion. The anthracene groups of adjacent molecules align with one another to form sheets that are perpendicular to the long molecular axis (monoclinic unit cell). Such packing maximizes the two-dimensional  $\pi$  interactions between the molecules, and is slightly different to that of other long acenes, for example, pentacene, which show slippage along the long molecular axis.<sup>[24]</sup>

The bias-stress effects and the shelf stability of the device are critical for the application of OSCs.<sup>[25]</sup> HPVAnt-based TF-FETs that were made on bare SiO<sub>2</sub>/Si have excellent stability after more than 20,000 operating cycles in vacuum ( $\mu^+ =$

$(1.01 \pm 0.09) \text{ cm}^2 \text{ V}^{-1} \text{ s}^{-1}$  see the Supporting Information), but are less stable when operating in air. However, the devices that were made on the PMMA-coated substrate demonstrated an almost constant mobility of  $(0.5 \pm 0.05) \text{ cm}^2 \text{ V}^{-1} \text{ s}^{-1}$  for more than 20000 cycles in air (continuous 18 h run). The shelf-life stability of the TF-FETs after storage of the unencapsulated devices under ambient conditions (exposed to air and light) is excellent (the  $\mu$  value drops from  $1 \text{ cm}^2 \text{ V}^{-1} \text{ s}^{-1}$  to  $0.9 \text{ cm}^2 \text{ V}^{-1} \text{ s}^{-1}$  and  $0.84 \text{ cm}^2 \text{ V}^{-1} \text{ s}^{-1}$  over 3 and 12 months storage, respectively). Besides excellent transistor characteristics, almost all devices produce blue EL that is modulated by a gate voltage ( $V_G$ , Figure 2b). As in other OLET devices with a single-carrier majority channel, the emission zone is concentrated in the vicinity of the drain electrode.<sup>[3b]</sup> Because of the top-contact configuration, most of the emitted light must be buried under the drain; the intense blue emission is nevertheless clearly visible at the electrode edges.

Unlike in other single-layer OLETs, the emission of HPVAnt is not subject to a “fatigue” effect, that is, the emission does not fade out during continuous operation (see the video in the Supporting Information). We note that only a few blue-emitting OLETs have been reported to date;<sup>[26]</sup> the highest mobility, which was measured for 4,4'-distyrylbi-phenyl, was  $0.01 \text{ cm}^2 \text{ V}^{-1} \text{ s}^{-1}$  (PLQY = 20 %).<sup>[26b]</sup> We also studied the performance of HPVAnt in single-crystal devices. Crystals of HPVAnt were grown from the vapor phase in a flow of Ar.<sup>[27]</sup> Single-crystal FET (SC-FET) structures were prepared by laminating the crystals onto a PMMA-coated Si/SiO<sub>2</sub> substrate, and then the source and drain electrodes were deposited by evaporating Au through a shadow mask. As a result of the relatively large thickness of the crystals (a few μm), the top metal contacts are located far from the charge accumulation zone (HPVAnt/PMMA interface), which leads to a large contact resistance.

Depending on crystal thickness, the buffer layer (MoO<sub>3</sub>, CsF), and the electrode (Au or Ca), the  $\mu^+$  value was in the range of  $0.75$ – $2.62 \text{ cm}^2 \text{ V}^{-1} \text{ s}^{-1}$ . Remarkably, the current density in a saturation regime (more than  $40 \text{ kA cm}^{-2}$ ) exceeds that of the rubrene-based SC-FET devices<sup>[3f]</sup> (see the Supporting Information). Furthermore, an ambipolar behavior with electron mobility in the range of  $0.04$ – $0.13 \text{ cm}^2 \text{ V}^{-1} \text{ s}^{-1}$  was measured for the HPVAnt/PMMA SC-FET (see the Supporting Information).

We also investigated the light-emitting properties of HPVAnt in SC-FET configuration. The optical image of the device and PL of the single crystal are shown in Figure 4a,b. The EL spectrum closely resembles the PL spectrum; the emission band is somewhat broadened, but the  $\lambda_{\text{max}}$  (490 nm) is not shifted (Figure 4c). Figure 4d shows optical images of EL that were taken of the surface of a device operating at fixed gate voltage ( $-200 \text{ V}$ ) while sweeping the drain-source voltage ( $V_{\text{DS}}$ ) between  $0 \text{ V}$  and  $-200 \text{ V}$ . At a lower operating bias, the EL is dominated by hole transport and the emission zone is close to the drain electrode. However, increasing the electron injection at higher  $V_{\text{DS}}$  values progressively extends the light emission zone toward the source electrode, which confirms the ambipolarity of the device.



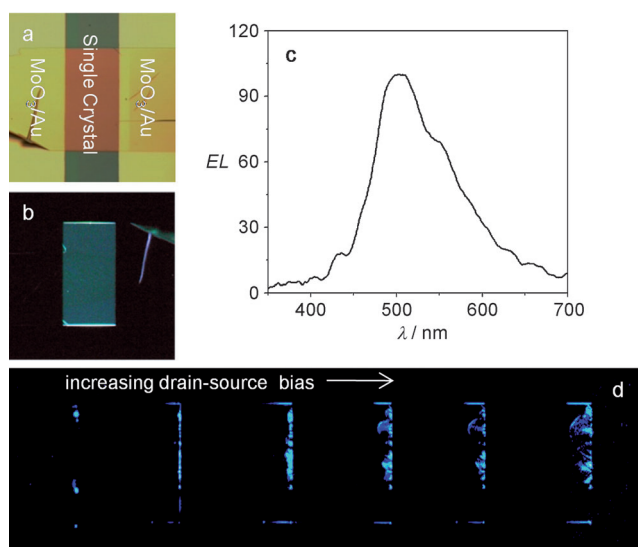


**Figure 4.** Light-emitting behavior of SC-FET: a) Optical image. b) PL image upon UV excitation. c) EL spectrum of biased device. d) Shift of the EL zone upon increasing bias.

In conclusion, we have demonstrated that the structurally simple hydrocarbon HPVAnt exhibits a unique combination of high field-effect mobility of up to  $1.5 \text{ cm}^2 \text{ V}^{-1} \text{ s}^{-1}$  in thin films ( $2.6 \text{ cm}^2 \text{ V}^{-1} \text{ s}^{-1}$  in single crystals), strong solid-state emission, and excellent operational stability in air. Both thin-film and single-crystal transistors emit bright-blue EL that is stable under continuous operation. To the best of our knowledge, this is the highest mobility OLET prepared to date. Importantly, the high PLQY of 70 % that was achieved for HPVAnt crystals disproves the common belief that the strong  $\pi$ - $\pi$  interactions that are required for high charge mobility necessarily lead to quenching of the luminescence in the solid state. This is likely attributable to the high energy of the excited state  $T_1$  relative to  $S_1$  ( $2T_1 > S_1$ ), which turns off emission quenching through singlet fission and, thus, outlines a new principle for the design of emissive crystalline OSCs.

Received: November 22, 2011

Revised: January 11, 2012

Published online: March 2, 2012

**Keywords:** anthracenes · luminescence · semiconductors · singlet fission · transistors

[1] S. R. Forrest, *Nature* **2004**, 428, 911.

[2] M. C. Gather, A. Kohnen, K. Meerholz, *Adv. Mater.* **2011**, 23, 233.

[3] a) A. Hepp, H. Heil, W. Weise, M. Ahles, R. Schmechel, H. von Seggern, *Phys. Rev. Lett.* **2003**, 91, 157406; b) F. Cicoira, C. Santato, *Adv. Funct. Mater.* **2007**, 17, 3421; c) R. Capelli, S. Toffanin, G. Generali, H. Usta, A. Facchetti, M. Muccini, *Nat. Mater.* **2010**, 9, 496; d) C. Santato, F. Cicoira, R. Martel, *Nat. Photonics* **2011**, 5, 392; e) S. Z. Bisri, T. Takenobu, K. Sawabe, S. Tsuda, Y. Yomogida, T. Yamao, S. Hotta, C. Adachi, Y. Iwasa, *Adv. Mater.* **2011**, 23, 2753; f) T. Takenobu, S. Z. Bisri, T. Takahashi, M. Yahiro, C. Adachi, Y. Iwasa, *Phys. Rev. Lett.* **2008**, 100, 066601.

- [4] a) I. D. W. Samuel, G. A. Turnbull, *Chem. Rev.* **2007**, 107, 1272; b) E. B. Namdas, M. Tong, P. Ledochowitsch, S. R. Mednick, J. D. Yuen, D. Moses, A. J. Heeger, *Adv. Mater.* **2009**, 21, 799.
- [5] a) I. F. Perepichka, D. F. Perepichka, H. Meng, F. Wudl, *Adv. Mater.* **2005**, 17, 2281–2305; b) P. Taranekekar, Q. Qiao, H. Jiang, K. S. Schanze, J. R. Reynolds, *J. Am. Chem. Soc.* **2007**, 129, 8958.
- [6] a) M. B. Smith, J. Michl, *Chem. Rev.* **2010**, 110, 6891; b) H. Najafov, B. Lee, Q. Zhou, L. C. Feldman, V. Podzorov, *Nat. Mater.* **2010**, 9, 938.
- [7] W. Wang, T. Lin, M. Wang, T.-X. Liu, L. Ren, D. Chen, S. Huang, *J. Phys. Chem. B* **2010**, 114, 5983.
- [8] a) R. Deans, J. Kim, M. R. Machacek, T. M. Swager, *J. Am. Chem. Soc.* **2000**, 122, 8565–8566; b) J. Luo, Z. Xie, J. W. Y. Lam, L. Cheng, H. Chen, C. Qiu, H. S. Kwok, X. Zhan, Y. Liu, D. Zhu, B. Z. Tang, *Chem. Commun.* **2001**, 1740.
- [9] R. Katoh, K. Suzuki, A. Furube, M. Kotani, K. Tokumaru, *J. Phys. Chem. C* **2009**, 113, 2961.
- [10] D. J. Gundlach, J. A. Nichols, L. Zhou, T. N. Jackson, *Appl. Phys. Lett.* **2002**, 80, 2925.
- [11] S. H. Lim, T. G. Bjorklund, F. C. Spano, C. J. Bardeen, *Phys. Rev. Lett.* **2004**, 92, 107402.
- [12] a) E. Menard, V. Podzorov, S.-H. Hur, A. Gaur, M. E. Gershenson, J. A. Rogers, *Adv. Mater.* **2004**, 16, 2097; b) J. Takeya, T. Nishikawa, T. Takenobu, S. Kobayashi, Y. Iwasa, T. Mitani, C. Goldmann, C. Krellner, B. Batlogg, *Appl. Phys. Lett.* **2004**, 85, 5078.
- [13] H. Klauk, M. Halik, U. Zschieschang, G. Schmid, W. Radlik, W. Weber, *J. Appl. Phys.* **2002**, 92, 5259.
- [14] a) W. Wu, Y. Liu, D. Zhu, *Chem. Soc. Rev.* **2010**, 39, 1489; b) J. E. Anthony, A. Facchetti, M. Heeney, S. R. Marder, X. Zhan, *Adv. Mater.* **2010**, 22, 3876; c) S. Allard, M. Forster, B. Souharce, H. Thiem, U. Scherf, *Angew. Chem.* **2008**, 120, 4138; *Angew. Chem. Int. Ed.* **2008**, 47, 4070; d) A. R. Murphy, J. M. J. Frechet, *Chem. Rev.* **2007**, 107, 1066.
- [15] M. J. Kang, I. Doi, H. Mori, E. Miyazaki, K. Takimiya, M. Ikeda, H. Kuwabara, *Adv. Mater.* **2011**, 23, 1222.
- [16] A. N. Sokolov, S. Atahan-Evrenk, R. Mondal, H. B. Akkerman, R. S. Sanchez-Carrera, S. Granados-Focil, J. Schrier, S. C. B. Mannsfeld, A. P. Zoombelt, Z. N. Bao, A. Aspuru-Guzik, *Nat. Commun.* **2011**, 2, 437.
- [17] a) H. Meng, F. Sun, M. B. Goldfinger, F. Gao, D. J. Londono, W. J. Marshall, G. S. Blackman, K. D. Dobbs, D. E. Keys, *J. Am. Chem. Soc.* **2006**, 128, 9304; b) H. Klauk, U. Zschieschang, R. T. Weitz, H. Meng, F. Sun, G. Nunes, D. E. Keys, C. R. Fincher, Z. Xiang, *Adv. Mater.* **2007**, 19, 3882; c) F. Cicoira, C. Santato, A. Dadvand, C. Harnagea, A. Pignolet, P. Bellutti, Z. Xiang, F. Rosei, H. Meng, D. F. Perepichka, *J. Mater. Chem.* **2008**, 18, 158.
- [18] The fluorescence of HPVAnt decay biexponentially with approximate lifetimes of  $\tau_1 = 6.7 \text{ ns}$  (72 %) and  $\tau_2 = 27 \text{ ns}$  (28 %) in solution,  $\tau_1 = 9.2 \text{ ns}$  (69 %) and  $\tau_2 = 20.5 \text{ ns}$  (31 %) in crystals, and  $\tau_1 = 1.4 \text{ ns}$  (79 %) and  $\tau_2 = 6.3 \text{ ns}$  (21 %) in thin films (see the Supporting Information). Similar lifetimes and biexponential decay was shown for 2-styrylanthracene: G. Bartocci, U. Mazzucato, A. Spalletti, F. Elise, *Spectrochim. Acta Part A* **1990**, 46, 413.
- [19] The  $S_1$  state lies between the highest-energy absorption peak (394 nm, 3.15 eV) and lowest-energy emission peak (423 nm, 2.94 eV). A cross-point of the absorption and emission spectra occurs at 406 nm (3.06 eV).
- [20] J. R. Shaw, R. T. Webb, R. H. Schmehl, *J. Am. Chem. Soc.* **1990**, 112, 1117.
- [21] R. W. T. Higgins, A. P. Monkman, H. G. Nothofer, U. Scherf, *Appl. Phys. Lett.* **2001**, 79, 857.
- [22] N. E. Gruhn, D. A. da Silva Filho, T. G. Bill, M. Malagoli, V. Coropceanu, A. Kahn, J. L. Bredas, *J. Am. Chem. Soc.* **2002**, 124, 7918.

- [23] A. A. Virkar, S. Mannsfeld, Z. Bao, N. Stingelin, *Adv. Mater.* **2010**, 22, 3857.
- [24] J. Anthony, *Angew. Chem.* **2008**, 120, 460; *Angew. Chem. Int. Ed.* **2008**, 47, 452.
- [25] H. Sirringhaus, *Adv. Mater.* **2009**, 21, 3859.
- [26] a) T. Oyamada, C. H. Chang, T. C. Chao, F. C. Fang, C. C. Wu, K. T. Wong, H. Sasabe, C. Adachi, *J. Phys. Chem. C* **2007**, 111, 108; b) T. Sakanoue, M. Yahiro, C. Adachi, H. Uchiuzou, T. Takahashi, A. Toshimitsu, *Appl. Phys. Lett.* **2007**, 90, 171118; c) H. Nakanotani, R. Kabe, M. Yahiro, T. Takenobu, Y. Iwasa, H. Adachi, *Appl. Phys. Express* **2008**, 1, 091801.
- [27] L. B. Roberson, J. Kowalik, L. M. Tolbert, C. Kloc, R. Zeis, X. Chi, R. Fleming, C. Wilkins, *J. Am. Chem. Soc.* **2005**, 127, 3069.
- [28] The shoulder at 410 nm in the solution absorption spectrum was earlier explained by equilibrium with the *s*-cis conformer: G. Fischer, E. Fischer, *J. Phys. Chem.* **1981**, 85, 2611.
-